MHJ
LUMORA JOURNALS

Multidisciplinary Healthcare Journal
Vol. 1, No. 6 (2025) · e-ISSN 3152-8775

Original Article · DOI: not registered

Whole-body physiologically based pharmacokinetic modelling of theophylline evaluated against open concentration–time data and applied to a 2022 age-standardised Saudi BMI scenario using evidence published by 2025

Fatema Alawad[1,*], Abdullah Adel Bouzaid[2], Abdullah Yousef[3], Mohammad Dairi[4], Nadia Sharif[5], Ragdah Arif[6], Renas Haitham Barmandah[7]

Received	Acceptance date	Publication date
20 June 2025	25 June 2025	30 June 2025

[1] College of Medicine, King Faisal University, Al-Ahsa, Saudi Arabia
[2] Imam Abdulrahman bin Faisal University, Saudi Arabia
[3] Abdulrahman bin Faisal University, Dammam, Saudi Arabia
[4] College of Medicine, Umm Al-Qura University, Makkah, Saudi Arabia
[5] Hera General Hospital Mecca, Makkah, Saudi Arabia
[6] King Abdulaziz University Faculty of Medicine, Jeddah, Saudi Arabia
[7] King Saud bin Abdulaziz University for Health Sciences, Saudi Arabia

*** Correspondence:** Fatema Alawad, fatemalumora@gmail.com

ABSTRACT

Theophylline PBPK exploratory simulations

2022 age-standardised Saudi BMI scenario
Source published in 2024 | 3,000 virtual adults

Distribution evaluated; clearance qualification incomplete
Simulation results do not establish dosing recommendations

GRAPHICAL ABSTRACT

Background: Weight-based dosing scalars may give different theophylline exposures in obesity. We evaluated a whole-body PBPK model and compared dosing scalars in an explicitly hypothetical population scenario informed by Saudi BMI estimates published before 2026.

Methods: A 14-compartment model was estimated from Theoph data in 12 adults and evaluated against independent published group means. The former 2026-updated WHO inputs were replaced by the archived NCD-RisC 2024 publication dataset describing 2022 age-standardised BMI categories for Saudi Arabia. Sex-specific log-normal distributions and published height means generated 3,000 virtual adults. A 5 mg/kg intravenous loading infusion and 0.4 mg/kg/h maintenance infusion were simulated under four dosing scalars, with 200 bootstrap uncertainty replicates. These age-standardised inputs define a comparison scenario, not the crude distribution of current Saudi patients.

Results: Held-out concentrations had an absolute average fold error of 1.304. Eight of 14 external metrics met the prespecified 0.8–1.25 criterion; all seven distribution-volume metrics met it, but clearance was underpredicted. In the revised population scenario, 42.7% had obesity and 8.5% had BMI ≥40 kg/m². In that highest class, 74.4% were within 10–20 mg/L at 72 h under TBW dosing (95% parameter uncertainty interval 49.0–98.0), with 22.8% above 20 mg/L. AdjBW gave 61.8% in range (43.9–81.4), 0.4% above and 37.8% below. IBW gave 13.4% in range. Loading with TBW or AdjBW placed all simulated adults in range under the model assumptions.

Conclusions: Changing the weight scalar materially changed simulated exposure. Distribution-volume agreement supports exploratory loading comparisons, while failed clearance qualification prevents reliable maintenance-dose recommendations. Apparent 100% attainment is conditional on the model and incomplete variability representation, not a probability of success in patients. Prospective clinical evaluation and therapeutic drug monitoring remain necessary.

Keywords: physiologically based pharmacokinetics; obesity; theophylline; dosing scalar; Saudi Arabia; model qualification

Cite as: Alawad F, Bouzaid AA, Yousef A, Dairi M, Sharif N, Arif R, et al. Whole-body physiologically based pharmacokinetic modelling of theophylline evaluated against open concentration–time data and applied to a 2022 age-standardised Saudi BMI scenario using evidence published by 2025. Multidisciplinary Healthcare Journal. 2025;1(6):MHJ-2026-000375. © The authors. Published open access under the Creative Commons Attribution 4.0 International licence (CC BY 4.0), https://creativecommons.org/licenses/by/4.0/.

1. Introduction

Saudi obesity estimates differ by measurement and standardisation. A 2020 telephone survey estimated weighted obesity prevalence at about one quarter [1], while subsequent surveillance described self-reported trends [2]. The NCD-RisC analysis published in 2024 estimated age-standardised 2022 obesity at 38.1% for men and 48.3% for women in Saudi Arabia [3]. Age-standardised estimates must not be interpreted as crude national prevalence. We use them solely to define a reproducible historical simulation scenario.

Obesity changes body composition, blood flows and drug disposition, and the effect is drug-specific [4, 5]. A single weight descriptor cannot therefore be assumed to perform well for all drugs. Simulation can explore consequences of explicit physiological assumptions, provided that extrapolation and uncertainty are distinguished from clinical validation.

Theophylline is a useful test case for this problem. It is a methylxanthine bronchodilator with a narrow therapeutic window, conventionally 10–20 mg/L, and adverse effects that become more frequent as plasma concentrations rise [6]. Its role has narrowed as inhaled therapies have improved, but it remains a low-cost option for airway disease [6]. Saudi asthma management guidance is updated regularly [7], and theophylline continues to be evaluated as an add-on therapy in chronic obstructive pulmonary disease [8]. Theophylline also has unusually rich obesity pharmacokinetic data. In the late 1970s and 1980s, several groups reported its distribution volume and clearance in obese and non-obese adults [9, 10, 11, 12, 13, 14]. These studies did not agree on the best weight descriptor. Some favoured TBW for loading doses [9], others IBW [11, 13], and one fitted an empirical power function of TBW [12]. They supply independent clinical observations that a mechanistic model

can be tested against, but they do not show how dosing rules would perform across the BMI distribution of the present Saudi population.

PBPK models separate drug properties from organ volumes, flows and tissue composition [15]. Obesity applications include oncology and paediatric examples published by 2025 [16, 17]. Regulatory guidance recommends explicit reporting of context, inputs, estimation and predictive performance [18]. Here, the model is evaluated against observed data before exploratory application; unsuccessful clearance qualification is retained as a substantive limitation.

We aimed to evaluate a theophylline PBPK model against open individual data and independent obesity summaries, then compare weight scalars in a 2022 age-standardised Saudi BMI scenario. This is a simulation-based comparison of model behaviour, not development of a clinical dosing recommendation.

2. Methods

2.1 Design, context of use and reporting

The study has model estimation, external evaluation and exploratory application stages. Reporting follows FDA recommendations for PBPK analyses [18]. The replacement of population inputs by the archived 2024 release was an editorial correction made after the original analysis, not a prespecified change. No new human participants were enrolled.

2.2 Data sources

The drug, physiology and individual concentration inputs were retrieved on 6 November 2026. During editorial correction, the 2026-updated WHO BMI files were removed and replaced by Saudi rows from the archived NCD-RisC 2024 dataset. The replacement files and extracted rows were preserved with checksums. Retrieval in 2026 is distinguished from the evidence publication date.

(i) Compound and system parameters came from the open-source R package httk, version 2.7.4 [19]. It provided the theophylline record (molecular weight, octanol:water partition coefficient, acid dissociation constant, fraction unbound in plasma, blood:plasma ratio, in vitro hepatocyte intrinsic clearance and fraction absorbed), human tissue composition data from Schmitt [20], tissue volumes, tissue blood flows [21] and the calibration regression of Pearce and colleagues [22].

(ii) Individual concentration–time data came from R datasets::Theoph. This is an open dataset of 12 adults who received a single oral theophylline dose of 3.1–5.86 mg/kg and had 11 serum samples each over about 25 h (132 samples in total). Body weights ranged from 54.6 to 86.4 kg.

(iii) External qualification targets were group means transcribed from four independent published studies of theophylline in obese and non-obese adults: Gal and colleagues (14 obese and 57 normal-weight adults) [9], Blouin and colleagues (12 markedly obese patients) [10], Rohrbaugh and colleagues (8 lean and 8 obese subjects) [11], and Rizzo and colleagues (40 asthmatic patients weighing 45–176 kg) [12]. None of these data were used to estimate model parameters.

(iv) The revised population inputs are sex-specific 2022 age-standardised prevalences of BMI <18.5, 25 to <30 and ≥30 kg/m² from the NCD-RisC Lancet 2024 archived country dataset [3]. These are standardised to a reference age distribution and are not crude resident-population prevalences. Published NCD-RisC height means of 167.7 cm for men and 155.9 cm for women were retained [23].

2.3 Model structure

The model comprised 14 flow-limited compartments: venous and arterial blood, lung, adipose tissue, bone, brain, gut, heart, kidney, liver, muscle, skin, spleen and a remainder compartment. A gut lumen depot was added for oral dosing. Gut and spleen drain into the liver through the portal vein. The reference total hepatic blood flow was 87.0 L/h, and the hepatic arterial flow was obtained by subtracting gut and spleen flows. The reference cardiac output was 336.0 L/h. The concentration in blood leaving each tissue was the tissue concen-

tration multiplied by the blood:plasma ratio and divided by the tissue:plasma partition coefficient (Kp). Elimination was hepatic and described by the well-stirred liver model. The unbound intrinsic clearance was scaled from the in vitro hepatocyte value using 110 × 106 hepatocytes per gram of liver and the predicted liver mass, after correction for binding in the incubation (fraction unbound in the incubation 0.955) [24]. Renal excretion of unchanged theophylline is minor and was absorbed into total clearance. Because every process was first order, the system was linear and was solved exactly with matrix exponentials rather than numerical integration.

2.4 Drug-specific inputs and partition coefficients

Table 1 lists the drug-specific inputs and their sources [24, 25, 26, 27, 28, 29]. Tissue Kp values were first predicted mechanistically with the Schmitt method [20], using membrane affinity estimated from lipophilicity [25]. They were then adjusted with the Pearce calibration regression, which is the default in httk and was developed to correct systematic bias of the uncalibrated Schmitt method [22]. Uncalibrated Kp values were retained as a sensitivity analysis.

Table 1. Drug-specific and system parameters of the theophylline physiologically based pharmacokinetic model.

Parameter	Value	Unit	Source
Molecular weight	180.2	g/mol	OPERA prediction (httk 2.7.4)
log P (octanol:water)	-0.02	-	OPERA prediction (httk 2.7.4)
pKa (acidic)	7.82	-	ChemAxon prediction (httk 2.7.4)
Fraction unbound in plasma	0.61	-	Lombardo et al. [33]
Blood:plasma ratio	1.33	-	Paixão et al. [35]
Hepatocyte intrinsic clearance (in vitro)	0.78	μL/min/10^6 cells	Wood et al. [34]
Fraction unbound in hepatocyte incubation	0.955	-	Kilford et al. equation [31]
Fraction absorbed	1.0	-	Varma et al. [36]
Hepatocellularity	110	10^6 cells/g liver	httk default [26]
Clearance scaling factor (SF)	0.471 (0.398–0.533)	-	Estimated, Theoph data
Between-subject SD of log SF	0.267 (0.114–0.369)	-	Estimated, Theoph data
Global partition-coefficient scalar	0.571 (0.517–0.625)	-	Estimated, Theoph data
Absorption rate constant	1.08	1/h	Estimated, Theoph data
Reference cardiac output	336.0	L/h	httk physiology, 70 kg [26]
Reference total hepatic blood flow	87.0	L/h	Davies and Morris [28]
Reference lean body weight	56.1	kg	Janmahasatian et al. [37]

Values in parentheses are 95% bootstrap confidence intervals (500 resamples of subjects). log P, logarithm of the octanol:water partition coefficient; pKa, negative logarithm of the acid dissociation constant; SD, standard deviation; SF, empirical multiplier applied to the in vitro–in vivo extrapolated intrinsic clearance. The reference individual is a man weighing 70 kg with a height of 1.76 m.

2.5 Body composition and scaling to obesity

For each individual, LBW was calculated with the Janmahasatian equations [30], IBW with the Devine equations [31], and AdjBW as IBW plus 0.4 times the excess of TBW over IBW. Fat mass was TBW minus LBW. The volumes of all lean organs, plasma volume and the remainder compartment were scaled in proportion to LBW relative to the reference LBW of 56.1 kg. Adipose volume was calculated from fat mass and adipose density. Lean-tissue blood flows were scaled with the 0.75 power of the LBW ratio. Adipose blood flow was as-

sumed proportional to adipose volume, and cardiac output was the sum of tissue flows. Hepatic intrinsic clearance therefore rose with liver mass and, through it, with LBW. This scaling assumption was tested in external qualification rather than fitted.

2.6 Middle-out parameter estimation and internal evaluation

A purely bottom-up model was first simulated with no empirical adjustment. Three parameters were then estimated for each Theoph subject by minimising squared log-residuals: the absorption rate constant, the clearance scaling factor and a single global scalar applied to all Kp values. The partition-coefficient scalar was not prespecified. It was added post hoc, after the bottom-up model was seen to overpredict distribution volume in these data, and it scales all tissues equally; obese-population data were never used to choose or estimate it. The pre-dose sample of each subject was excluded, leaving 120 post-dose observations. Each subject's own body weight was used; height was not recorded and was set to 1.76 m. Population values were geometric means across subjects, and between-subject variability of clearance was the standard deviation of the log scaling factor. Predictive performance was assessed by leave-one-subject-out cross-validation. Each subject's profile was predicted from population values estimated on the remaining 11 subjects, and we summarised the average fold error, the absolute average fold error, the proportion of concentrations within two-fold and 1.25-fold, and predicted-to-observed ratios of area under the curve and peak concentration [32]. Parameter uncertainty was quantified by bootstrapping subjects (500 resamples).

2.7 External qualification in obesity

The qualified model was used, without further adjustment, to simulate typical men (1.76 m) and women (1.63 m) matching the body-size characteristics reported in each external study, and sex-averaged predictions were compared with the published group means. For the study by Gal and colleagues, the mean ratio of TBW to IBW in the obese group (2.02) was derived from the reported volume per kg of TBW and per kg of IBW. For the study by Blouin and colleagues, the corresponding ratio (1.86) was derived from the reported clearance values. For the study by Rohrbaugh and colleagues, mean body weights (57.0 kg lean and 88.8 kg obese) were derived from the reported volumes in litres and per kg. The apparent distribution volume during the terminal phase was compared with the published apparent volumes. We also compared predicted distribution volume for typical men (1.72 m) and women (1.60 m) across TBW from 45 to 176 kg with the empirical power function reported by Rizzo and colleagues (volume = $1.29 \times \mathrm{TBW}^{0.74}$). The prespecified criterion for adequate prediction of a group mean was a predicted-to-observed ratio between 0.8 and 1.25; ratios within two-fold were also reported.

2.8 Virtual Saudi adult population

For each sex, a log-normal BMI distribution was fitted to the three archived 2022 age-standardised category probabilities. Height was drawn around the published sex-specific mean with assumed SD 6.5 cm and truncation 140–200 cm; BMI was truncated to 16–70 kg/m². We generated 1,500 virtual men and 1,500 virtual women. The resulting 50:50 mixture is an assumed comparison scenario, not a demographic representation of Saudi Arabia. The three category inputs do not fully determine the tails of the true BMI distribution; the log-normal assumption is additional.

2.9 Dosing scenarios, outcomes and uncertainty

Each virtual adult received an intravenous loading dose of 5 mg/kg over 0.5 h followed by a continuous infusion of 0.4 mg/kg/h. In turn, the weight in mg/kg was TBW, AdjBW, IBW or LBW. The primary outcomes were the proportions of adults with plasma concentrations of 10–20 mg/L at the end of the loading infusion and after 72 h of maintenance. Secondary outcomes were the proportions above 20 mg/L and below 10 mg/L, analysed overall and by BMI class (below 25, 25–29.9, 30–34.9, 35–39.9 and 40 $\mathrm{kg/m^2}$ or more). A narrower range of 5–15 mg/L was used as a sensitivity analysis. Parameter uncertainty was propagated by re-simulating 200 bootstrap replicates of the population clearance scaling factor, its variability and the partition-coefficient scalar on random subsamples of 600 virtual adults. The 2.5th and 97.5th percentiles across replicates were reported as 95% uncertainty intervals. Local sensitivity analyses in a reference woman with a BMI of 40 $\mathrm{kg/m^2}$ (97.3 kg,

1.56 m) varied the fraction unbound in plasma (±20%), the blood:plasma ratio (1.0 versus 1.33), log P (±1 unit), the acid dissociation constant (7.82 versus 8.8) and the clearance scaling factor (95% confidence limits).

2.10 Software

All analyses were performed in Python 3.13 with NumPy 2.5.3, SciPy 1.18.1 (matrix exponentials, least-squares and Nelder–Mead optimisation), pandas 2.3.3 and Matplotlib 3.11.2. R data objects were read with the rdata package. A single script reads only the frozen inputs and regenerates every number, table and figure.

3. Results

3.1 Bottom-up prediction and partition coefficients

Without empirical adjustment, the model predicted a plasma clearance of 5.62 L/h and a steady-state volume of 0.672 L/kg for the 70-kg reference man. In leave-out comparison with the Theoph data, bottom-up predictions showed an average fold error of 0.559 and an absolute average fold error of 1.898, with only 61.7% of concentrations within two-fold. The uncalibrated Schmitt method predicted an adipose Kp of 0.955. The Pearce calibration lowered this to 0.46 but raised the liver and kidney values above 2 (Table 2).

Table 2. Predicted tissue:plasma partition coefficients of theophylline.

Tissue	Schmitt, uncalibrated	Schmitt with Pearce calibration	Final model (scaled)
Adipose	0.955	0.46	0.263
Bone	0.281	0.402	0.23
Brain	1.154	0.735	0.42
Gut	0.678	1.03	0.589
Heart	0.645	0.966	0.552
Kidney	0.735	2.298	1.312
Liver	0.749	2.491	1.423
Lung	0.555	0.732	0.418
Muscle	0.573	0.658	0.376
Skin	1.272	0.93	0.531
Spleen	0.659	0.785	0.448
Remainder	0.878	0.876	0.5

Kp, tissue:plasma partition coefficient. The final model multiplies the calibrated values by the global partition-coefficient scalar of 0.571 estimated from the Theoph data. The calibration regression is not applied to the remainder compartment.

3.2 Middle-out estimation and internal evaluation

The estimated population clearance scaling factor was 0.471 (95% confidence interval 0.398–0.533). Between-subject variability in clearance corresponded to a coefficient of variation of 27.1%. The global partition-coefficient scalar was 0.571 (0.517–0.625), and individual estimates ranged from 0.422 to 0.803. The population absorption rate constant was 1.08 h^{-1}. Individual clearances ranged from 19.2 to 54.6 mL/h/kg (median 41.8 mL/h/kg), and the median individual steady-state volume was 0.432 L/kg. For the reference man, the qualified model predicted a clearance of 2.72 L/h, a steady-state volume of 0.428 L/kg and a terminal half-life of 7.7 h. The bottom-up clearance was therefore 2.07-fold higher than the clearance supported by the observed data.

In leave-one-subject-out prediction, the average fold error was 1.041 and the absolute average fold error was 1.304. Of the held-out concentrations, 93.3% fell within two-fold and 55.0% within 1.25-fold (Figure 1). The

geometric mean predicted-to-observed ratio of the area under the curve was 1.014 (range 0.61–1.39); all 12 subjects were within two-fold and 9 within 1.25-fold. For peak concentration, the geometric mean ratio was 0.947, with 9 subjects within 1.25-fold.

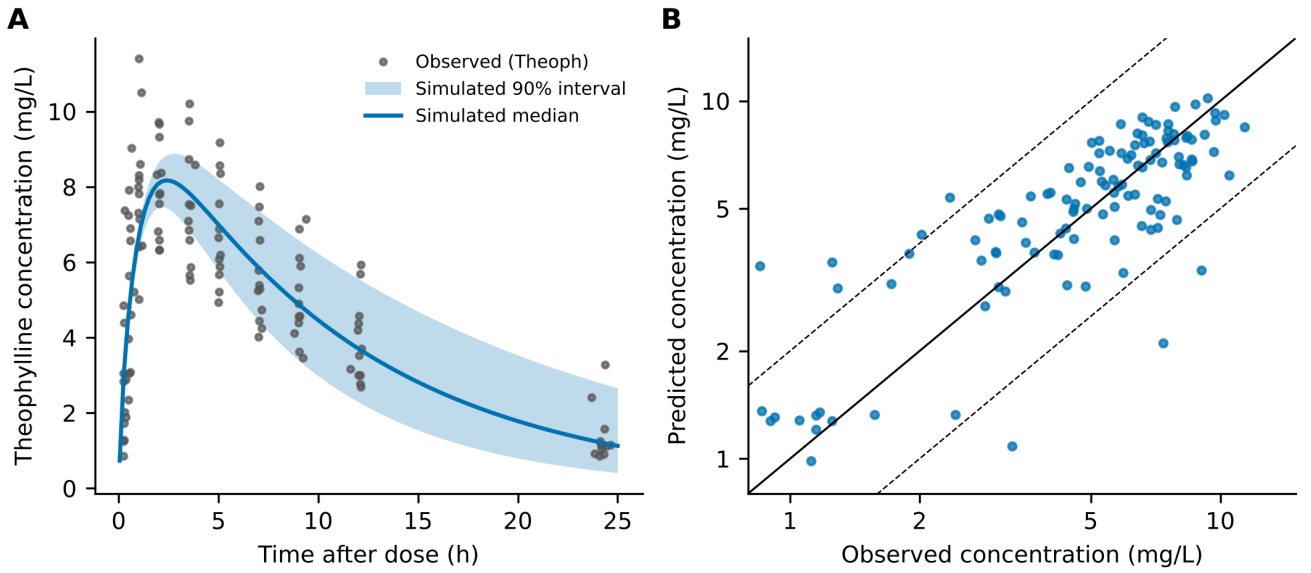


Figure 1. Internal qualification of the theophylline model against the open Theoph dataset. (A) Observed serum concentrations after a single oral dose (points; 12 adults) with the median and 90% interval of 200 simulated adults of similar body weight receiving 4.5 mg/kg. (B) Leave-one-subject-out predicted versus observed concentrations on logarithmic axes; the solid line is identity and the dashed lines mark two-fold limits.

3.3 External qualification in obesity

Only 8 of 14 external metrics met the prespecified 0.8–1.25 prediction criterion. All seven volume metrics met that criterion; clearance was systematically underpredicted, with ratios about 0.56–0.79. All metrics happened to lie within the secondary two-fold range, but that broader result does not override failed prespecified clearance qualification. The model is therefore partially evaluated for distribution and insufficiently qualified for absolute maintenance exposure. The volume comparison with the Rizzo function and the partition-coefficient sensitivity remain descriptive (Table 3 and Figure 2).

Table 3. External qualification of the theophylline model against independent published obese and non-obese adult studies.

Study (group)	Metric	Observed	Predicted	Ratio
Gal 1978 (normal)	Vd, L/kg TBW	0.482	0.417	0.866
Gal 1978 (normal)	CL, mL/h/kg IBW	63.0	35.524	0.564
Gal 1978 (normal)	t1/2, h	6.0	8.182	1.364
Gal 1978 (obese)	Vd, L/kg TBW	0.382	0.38	0.995
Gal 1978 (obese)	Vd, L/kg IBW	0.77	0.766	0.995
Gal 1978 (obese)	CL, mL/h/kg TBW	32.8	25.247	0.77
Gal 1978 (obese)	CL, mL/h/kg IBW	64.1	50.89	0.794
Gal 1978 (obese)	t1/2, h	8.6	10.47	1.217
Blouin 1980 (obese, no heart failure)	CL, mL/h/kg TBW	34.5	26.387	0.765
Blouin 1980 (obese, no heart failure)	CL, mL/h/kg IBW	64.3	49.179	0.765

Study (group)	Metric	Observed	Predicted	Ratio
Rohrbaugh 1982 (lean)	Vd, L/kg TBW	0.472	0.423	0.896
Rohrbaugh 1982 (obese)	Vd, L/kg TBW	0.321	0.4	1.246
Rohrbaugh 1982 (lean)	Vd, L	26.9	24.106	0.896
Rohrbaugh 1982 (obese)	Vd, L	28.5	35.505	1.246

Ratio, predicted divided by observed group mean. CL, total plasma clearance; IBW, ideal body weight; t1/2, terminal elimination half-life; TBW, total body weight; Vd, apparent volume of distribution (model value: terminal-phase volume). Observed values are group means from the cited abstracts [9, 10, 11]; none were used for parameter estimation.

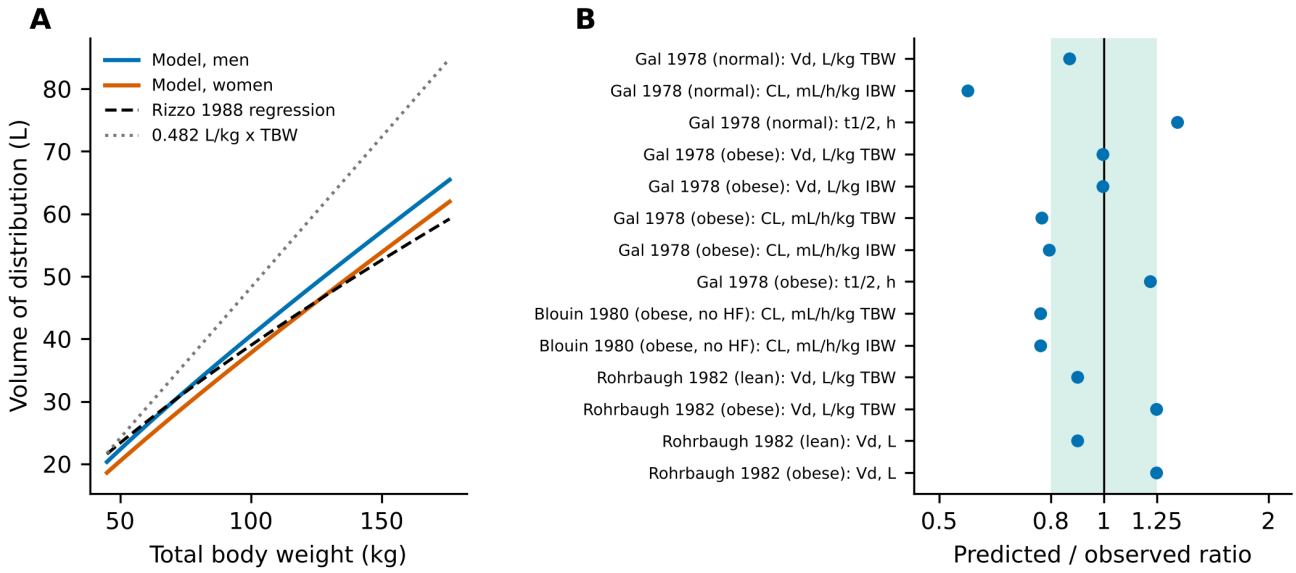


Figure 2. External qualification of predicted theophylline disposition across body size. (A) Predicted terminal-phase volume of distribution for typical men (1.72 m) and women (1.60 m) across total body weight (TBW), compared with the published power function of Rizzo and colleagues and with simple proportional scaling at 0.482 L/kg. (B) Predicted-to-observed ratios for 14 published group means; the shaded band marks 0.8–1.25. CL, clearance; HF, heart failure; IBW, ideal body weight; t1/2, half-life; Vd, volume of distribution.

3.4 Virtual Saudi population

The revised log-normal scenarios fitted prevalences of BMI ≥25 and ≥30 kg/m² of 72.2% and 38.4% in men, versus archived inputs 72.7% and 38.1%, and 75.2% and 48.6% in women, versus 75.8% and 48.3%. Median fitted BMI was 28.2 and 29.7 kg/m². The fitted ≥40 kg/m² tails were 4.5% and 12.2%; these are model-derived tails, not observed national prevalence. The 3,000 virtual adults had 42.7% obesity, 8.5% BMI ≥40 and median weight 75.5 kg (5th–95th percentile 49.9–113.7).

Revised disposition summaries are shown in Table 4. Across the lowest to highest BMI class, median Vss/TBW decreased from 0.422 to 0.372 L/kg, CL/TBW from 35.700 to 24.387 mL/h/kg, while CL/IBW increased from 36.401 to 53.827 mL/h/kg. Median terminal half-life increased from 8.153 to 10.642 h. These are model predictions under specified physiology and variability assumptions.

Table 4. Predicted theophylline disposition in the virtual Saudi adult population by body-mass-index class.

BMI	n	TBW kg	IBW kg	LBW kg	Vss L	CL L/h	t1/2 h	Vss/TBW (L/kg)	CL/TBW (mL/h/kg)	CL/IBW (mL/h/kg)
<25	814	59.1	58.9	44.4	24.64	2.061	8.15	0.422	35.700	36.401

BMI	n	TBW kg	IBW kg	LBW kg	Vss L	CL L/h	t1/2 h	Vss/TBW (L/kg)	CL/TBW (mL/h/kg)	CL/IBW (mL/h/kg)
25-29.9	904	72.5	57.6	50.8	29.41	2.390	8.61	0.411	32.847	42.132
30-34.9	664	84.3	56.6	52.6	33.55	2.501	9.25	0.401	29.803	45.046
35-39.9	364	96.3	54.2	51.2	36.77	2.585	10.03	0.380	26.724	46.704
>=40	254	112.9	51.1	53.9	42.53	2.735	10.64	0.372	24.387	53.827

Values are medians. BMI, body mass index; CL, total plasma clearance; IBW, ideal body weight; LBW, lean body weight; n, number of virtual adults; t1/2, terminal half-life; TBW, total body weight; Vss, volume of distribution at steady state.

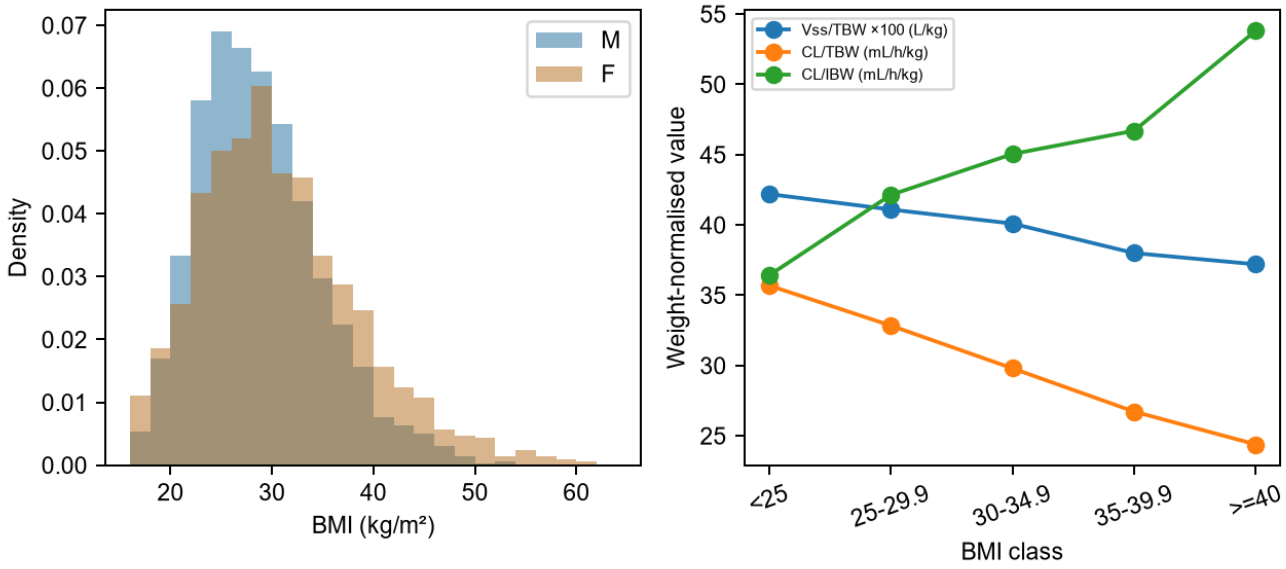


Figure 3. Revised 2022 age-standardised Saudi BMI simulation scenario. Left: simulated BMI in 1,500 virtual men and 1,500 virtual women; right: weight-normalised disposition summaries by BMI class. The mixture and distribution shapes are assumptions, not a sample of Saudi patients. Vss/TBW is multiplied by 100 for display, as labelled; clearance units are mL/h/kg.

3.5 Target attainment of dosing scalars

TBW- and AdjBW-based loading put 100% of the 3,000 simulated adults within 10–20 mg/L under the model assumptions. In the highest BMI class, median end-loading concentrations were 17.0 and 11.5 mg/L respectively; IBW gave 7.9 mg/L and no simulated individual in range. No claim of 100% clinical success follows: loading concentrations depend strongly on the represented distribution volumes, and interindividual partition-coefficient variability was not fully modelled.

At 72 h, TBW gave 71.7% in range overall, with 7.4% above 20 mg/L. At BMI ≥40, TBW gave 74.4% in range (95% parameter uncertainty interval 49.0–98.0) and 22.8% above 20 mg/L. AdjBW gave 60.1% in range overall; at BMI ≥40 it gave 61.8% in range (43.9–81.4), 0.4% above and 37.8% below 10 mg/L. IBW gave 13.4% in range in that class. These intervals propagate estimated parameter uncertainty and Monte Carlo subsampling, not all physiological or structural uncertainty.

Against the alternative 5–15 mg/L target, maintenance attainment at BMI ≥40 was TBW 40.5%, AdjBW 87.4%, IBW 93.7%, LBW 95.7%. The scalar ranking depends on the chosen target and unresolved clearance bias.

Table 5. Proportion of virtual Saudi adults within 10–20 mg/L by dosing scalar, overall and in the highest body-mass-index class.

Scalar	BMI	n	Loading in %	72 h in %	95% interval	72 h above %	72 h below %
TBW	all	3000	100.0	71.7	61.6–87.3	7.4	21.0
TBW	>=40	254	100.0	74.4	49.0–98.0	22.8	2.8
AdjBW	all	3000	100.0	60.1	37.2–73.3	1.1	38.9
AdjBW	>=40	254	100.0	61.8	43.9–81.4	0.4	37.8
IBW	all	3000	73.6	41.3	15.3–58.8	0.4	58.3
IBW	>=40	254	0.0	13.4	0.0–31.3	0.0	86.6
LBW	all	3000	47.9	22.0	0.5–46.4	0.0	77.9
LBW	>=40	254	0.0	20.1	0.0–39.7	0.0	79.9

Regimen: intravenous loading dose of 5 mg/kg over 0.5 h followed by 0.4 mg/kg/h, with mg/kg referring to the stated scalar. AdjBW, adjusted body weight (IBW + 0.4 × [TBW − IBW]); BMI, body mass index (kg/m2); IBW, ideal body weight; LBW, lean body weight; TBW, total body weight; UI, uncertainty interval across 200 bootstrap replicates of population parameters. Results for all BMI classes are given in the supplementary table.

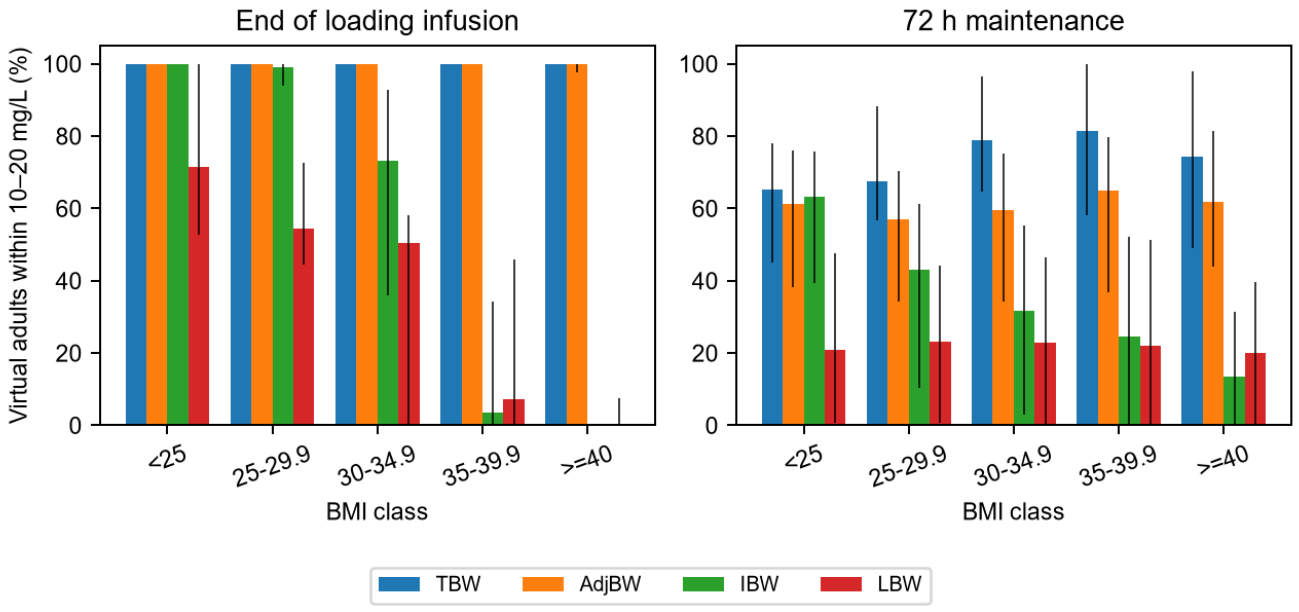


Figure 4. Revised target attainment by BMI class using archived pre-2026 evidence. Bars show proportions within 10–20 mg/L at end-loading and 72 h; vertical lines show 95% parameter-bootstrap intervals from 200 replicates. The results are conditional simulations rather than clinical dose recommendations.

3.6 Sensitivity analyses

In the reference woman with a BMI of 40 kg/m^2 (97.3 kg) receiving IBW-based dosing, the predicted steady-state volume was 36.5 L and clearance 2.36 L/h. Across the local sensitivity analyses, the 72-h concentration ranged from 6.9 to 10.2 mg/L, compared with a base value of 8.3 mg/L. The fraction unbound in plasma and the clearance scaling factor had the largest influence (72-h concentration 9.7 and 7.3 mg/L at the lower and

upper scaling-factor limits). Varying log P by one unit changed the steady-state volume from 29.189 to 59.773 L but changed the 72-h concentration little. The blood:plasma ratio had a negligible effect (steady-state volume 34.9 versus 36.5 L).

4. Discussion

4.1 Principal findings

The revised application replaces post-2025 population evidence with the archived 2024 release describing a 2022 age-standardised Saudi BMI scenario. The full model calculation and 200-replicate uncertainty analysis were rerun. Dosing scalars produced different exposures, but external evaluation supports distribution volumes more strongly than clearance. The failure of the prespecified clearance criterion limits maintenance interpretation; the simulation cannot establish which scalar is clinically optimal.

4.2 Comparison with previous studies

The results agree with the most consistent message of the clinical theophylline literature. Gal and colleagues found that distribution volume per kg of TBW was similar in obese and normal subjects and recommended TBW for loading [9]. The model reproduced their obese-group volume almost exactly and showed why: theophylline distributes mainly into body water, and adipose partitioning is low, but not negligible, relative to lean tissue. The empirical exponent of 0.74 reported by Rizzo and colleagues [12] lies between proportional scaling and no scaling, and the model's exponent of 0.87 kept predicted volumes within about 11% of their function over the full weight range. In contrast, the uncalibrated Schmitt partition coefficients implied more than proportional scaling of volume with TBW. With them, the model would have overpredicted volume by up to 68% at the highest weights. This finding is consistent with the known bias of the uncalibrated method for hydrophilic compounds and with the purpose of the Pearce calibration [22]. The conclusion of Rohrbaugh and colleagues [11] that IBW should be used for loading was based on a smaller obese group with a lower volume per kg of TBW; the model predicted that group's volume 25% higher. Zahorska-Markiewicz and colleagues likewise favoured IBW [13]. Some of the disagreement among the historical studies may therefore reflect small samples and differences in body composition, which a mechanistic model can address directly.

Historical studies differ in smoking, disease and body size, which can affect theophylline clearance [10, 14, 34, 35]. The model underestimated clearance and did not resolve these covariates. Demographic scaling of liver mass cannot be assumed to capture obesity-related enzyme activity [15]. These differences remain unresolved rather than being corrected by labelling all predictions within two-fold.

The bottom-up clearance discrepancy illustrates the limitations of in vitro–in vivo extrapolation [27]. Empirical adjustment was reported transparently and obesity summaries were not used to fit parameters. That separation prevents direct reuse of the external targets for estimation, but does not make a model qualified when the prespecified criterion fails. The post hoc partition-coefficient scalar and the publication-cutoff correction are explicitly identified.

4.3 Implications for Saudi practice

The age-standardised scenario is relevant to methodological questions in Saudi settings but does not estimate the distribution or dosing needs of current patients. Loading comparisons depend on the assumed distribution model; maintenance comparisons are additionally biased by underpredicted clearance. Neither the simulated target proportions nor the apparent ranking should be used for patient-specific dose selection. Local observed concentrations, comorbidities, smoking and therapeutic drug monitoring are needed before a clinical application.

4.4 Strengths and limitations

Strengths include open inputs, separation of estimation from external evaluation, a reproducible archived pre-2026 population source, explicit reporting of failed qualification and rerunning the revised population scenario with parameter uncertainty.

Limitations include abstract-level historical external targets, absent height/sex/smoking covariates in Theoph, a post hoc global partition scalar, incomplete clearance qualification and unrepresented variability in organ partitioning. The BMI source is age-standardised, the 50:50 sex mixture and log-normal tails are assumed, height variability is assumed, and no age-specific prevalence weights are modelled. Bootstrap intervals omit important structural and physiological uncertainty. No Saudi patient concentration data were used to validate the model. The results describe conditional pharmacokinetic simulations, not efficacy or toxicity in patients.

4.5 Future research

Future work should use Saudi therapeutic drug monitoring data with measured height, weight, age, smoking, comorbidity and interacting medications. The clearance model should be evaluated and improved against independent observations before maintenance predictions are used clinically. An age-specific resident-population model could replace the present standardised comparison scenario.

5. Conclusions

A theophylline PBPK model reproduced published distribution volumes more closely than clearance. Reanalysis using the archived NCD-RisC 2024 evidence produced a 2022 age-standardised Saudi BMI comparison scenario. Weight scalars changed predicted exposure, but incomplete clearance qualification, assumed population structure and incomplete variability preclude clinical dosing recommendations.

Declarations

Funding: NA

Conflicts of Interest: NA

Institutional Review Board Statement: This study used only publicly available, de-identified data and published summary statistics; no human participants were recruited and no ethics approval was sought or claimed.

Informed Consent Statement: Not applicable (public de-identified data).

Data availability: Theoph individual concentration data, httk-derived physiology and compound inputs, published height estimates and archived NCD-RisC Lancet 2024 BMI country estimates were used. The archived population source is https://ncdrisc.org/archives.html, with Saudi 2022 rows from NCD_RisC_Lancet_2024_BMI_age_standardised_country.csv. Publication year is 2024; retrieval and revised calculation occurred in 2026. The former WHO 2026-updated input files are not used in the revised application.

Author Contributions: NA

References

[1] Althumiri NA, Basyouni MH, AlMousa N, AlJuwaysim MF, Almubark RA, BinDhim NF, et al. Obesity in Saudi Arabia in 2020: Prevalence, Distribution, and Its Current Association with Various Health Conditions. Healthcare (Basel). 2021;9(3):311. doi:10.3390/healthcare9030311

[2] Althumiri NA, Bindhim NF, Al-Rayes SA, Alumran A. Mapping Obesity Trends in Saudi Arabia: A Four-Year Description Study. Healthcare (Basel). 2024;12(20):2092. doi:10.3390/healthcare12202092

[3] NCD Risk Factor Collaboration (NCD-RisC). Worldwide trends in underweight and obesity from 1990 to 2022: a pooled analysis of 3663 population-representative studies with 222 million children, adolescents, and adults. Lancet. 2024;403(10431):1027-1050. doi:10.1016/S0140-6736(23)02750-2

[4] Hanley MJ, Abernethy DR, Greenblatt DJ. Effect of Obesity on the Pharmacokinetics of Drugs in Humans. Clin Pharmacokinet. 2010;49(2):71-87. doi:10.2165/11318100-000000000-00000

[5] van Valkengoed DW, Krekels EHJ, Knibbe CAJ. All You Need to Know About Allometric Scaling: An Integrative Review on the Theoretical Basis, Empirical Evidence, and Application in Human Pharmacology. Clin Pharmacokinet. 2025;64(2):173-192. doi:10.1007/s40262-024-01444-6

[6] Barnes PJ. Theophylline. Am J Respir Crit Care Med. 2013;188(8):901-906. doi:10.1164/rccm.201302-0388PP

[7] Al-Moamary MS, Alhaider SA, Allehebi R, Idrees MM, Zeitouni MO, Al Ghobain MO, et al. The Saudi initiative for asthma – 2024 update: Guidelines for the diagnosis and management of asthma in adults and children. Ann Thorac Med. 2024;19(1):1-55. doi:10.4103/atm.atm_248_23

[8] Yang Q, Tang P, Zhang X. Effects of additional oral theophylline with inhaled therapy in patients with stable chronic obstructive pulmonary disease: A systematic review and meta-analysis. PLoS One. 2025;20(5):e0321984. doi:10.1371/journal.pone.0321984

[9] Gal P, Jusko WJ, Yurchak AM, Franklin BA. Theophylline disposition in obesity. Clin Pharmacol Ther. 1978;23(4):438-444. doi:10.1002/cpt1978234438

[10] Blouin RA, Elgert JF, Bauer LA. Theophylline clearance: Effect of marked obesity. Clin Pharmacol Ther. 1980;28(5):619-623. doi:10.1038/clpt.1980.212

[11] Rohrbaugh TM, Danish M, Ragni MC, Yaffe SJ. The effect of obesity on apparent volume of distribution of theophylline. Pediatr Pharmacol (New York). 1982;2(1):75-83. PMID: 7110759.

[12] Rizzo A, Mirabella A, Bonanno A. Effect of body weight on the volume of distribution of theophylline. Lung. 1988;166(5):269-276. doi:10.1007/BF02714057

[13] Zahorska-Markiewicz B, Waluga M, Zielinski M, Klin M. Pharmacokinetics of theophylline in obesity. Int J Clin Pharmacol Ther. 1996;34(9):393-5. PMID: 8880289.

[14] Jusko WJ, Gardner MJ, Mangione A, Schentag JJ, Koup JR, Vance JW. Factors affecting theophylline clearances: Age, tobacco, marijuana, cirrhosis, congestive heart failure, obesity, oral contraceptives, benzodiazepines, barbiturates, and ethanol. J Pharm Sci. 1979;68(11):1358-1366. doi:10.1002/jps.2600681106

[15] Ghobadi C, Johnson TN, Aarabi M, Almond LM, Allabi AC, Rowland-Yeo K, et al. Application of a Systems Approach to the Bottom-Up Assessment of Pharmacokinetics in Obese Patients. Clin Pharmacokinet. 2011;50(12):809-822. doi:10.2165/11594420-000000000-00000

[16] Burhanuddin K, Mohammed A, Burhanuddin NA, Badhan RKS. Precision Medicine in Oncology: Imatinib Dosing in the Obese Cancer Population Using Virtual Clinical Trials. CPT Pharmacometrics Syst Pharmacol. 2025;14(6):1050-1064. doi:10.1002/psp4.70018

[17] McCann S, Helfer VE, Balevic SJ, Muller WJ, van den Anker JN, Al-Uzri A, et al. Physiologically Based and Population Pharmacokinetic Modeling of Midazolam in Children With Obesity Using Real-World Data. Clin Transl Sci. 2025;18(5):e70247. doi:10.1111/cts.70247

[18] US Food and Drug Administration. Physiologically based pharmacokinetic analyses: format and content. Guidance for industry. Silver Spring (MD): FDA; 2018. Available from: https://www.fda.gov/media/101469/download

[19] Pearce RG, Setzer RW, Strope CL, Sipes NS, Wambaugh JF. httk: R Package for High-Throughput Toxicokinetics. J Stat Softw. 2017;79(4):1-26. doi:10.18637/jss.v079.i04

[20] Schmitt W. General approach for the calculation of tissue to plasma partition coefficients. Toxicol In Vitro. 2008;22(2):457-467. doi:10.1016/j.tiv.2007.09.010

[21] Davies B, Morris T. Physiological Parameters in Laboratory Animals and Humans. Pharm Res. 1993;10(7):1093-1095. doi:10.1023/A:1018943613122

[22] Pearce RG, Setzer RW, Davis JL, Wambaugh JF. Evaluation and calibration of high-throughput predictions of chemical distribution to tissues. J Pharmacokinet Pharmacodyn. 2017;44(6):549-565. doi:10.1007/s10928-017-9548-7

[23] NCD Risk Factor Collaboration (NCD-RisC). A century of trends in adult human height. eLife. 2016;5:e13410. doi:10.7554/eLife.13410

[24] Kilford PJ, Gertz M, Houston JB, Galetin A. Hepatocellular Binding of Drugs: Correction for Unbound Fraction in Hepatocyte Incubations Using Microsomal Binding or Drug Lipophilicity Data. Drug Metab Dispos. 2008;36(7):1194-1197. doi:10.1124/dmd.108.020834

[25] Yun YE, Edginton AN. Correlation-based prediction of tissue-to-plasma partition coefficients using readily available input parameters. Xenobiotica. 2013;43(10):839-852. doi:10.3109/00498254.2013.770182

[26] Lombardo F, Berellini G, Obach RS. Trend Analysis of a Database of Intravenous Pharmacokinetic Parameters in Humans for 1352 Drug Compounds. Drug Metab Dispos. 2018;46(11):1466-1477. doi:10.1124/dmd.118.082966

[27] Wood FL, Houston JB, Hallifax D. Clearance Prediction Methodology Needs Fundamental Improvement: Trends Common to Rat and Human Hepatocytes/Microsomes and Implications for Experimental Methodology. Drug Metab Dispos. 2017;45(11):1178-1188. doi:10.1124/dmd.117.077040

[28] Paixão P, Gouveia LF, Morais JAG. Prediction of the human oral bioavailability by using in vitro and in silico drug related parameters in a physiologically based absorption model. Int J Pharm. 2012;429(1-2):84-98. doi:10.1016/j.ijpharm.2012.03.019

[29] Varma MVS, Obach RS, Rotter C, Miller HR, Chang G, Steyn SJ, et al. Physicochemical Space for Optimum Oral Bioavailability: Contribution of Human Intestinal Absorption and First-Pass Elimination. J Med Chem. 2010;53(3):1098-1108. doi:10.1021/jm901371v

[30] Janmahasatian S, Duffull SB, Ash S, Ward LC, Byrne NM, Green B. Quantification of Lean Bodyweight. Clin Pharmacokinet. 2005;44(10):1051-1065. doi:10.2165/00003088-200544100-00004

[31] Pai MP, Paloucek FP. The Origin of the “Ideal” Body Weight Equations. Ann Pharmacother. 2000;34(9):1066-1069. doi:10.1345/aph.19381

[32] Guest EJ, Aarons L, Houston JB, Rostami-Hodjegan A, Galetin A. Critique of the Two-Fold Measure of Prediction Success for Ratios: Application for the Assessment of Drug-Drug Interactions. Drug Metab Dispos. 2011;39(2):170-173. doi:10.1124/dmd.110.036103

[33] Curry L, Alrubia S, Bois FY, Clayton R, El-Khateeb E, Johnson TN, et al. A guide to developing population files for physiologically-based pharmacokinetic modeling in the Simcyp Simulator. CPT Pharmacometrics Syst Pharmacol. 2024;13(9):1429-1447. doi:10.1002/psp4.13202

[34] Plowchalk DR, Rowland Yeo K. Prediction of drug clearance in a smoking population: modeling the impact of variable cigarette consumption on the induction of CYP1A2. Eur J Clin Pharmacol. 2012;68(6):951-960. doi:10.1007/s00228-011-1189-y

[35] Haraya K, Kato M, Chiba K, Sugiyama Y. Prediction of inter-individual variability on the pharmacokinetics of CYP1A2 substrates in non-smoking healthy volunteers. Drug Metab Pharmacokinet. 2016;31(4):276-284. doi:10.1016/j.dmpk.2016.03.003

[36] Hanke N, Frechen S, Moj D, Britz H, Eissing T, Wendl T, et al. PBPK Models for CYP3A4 and P-gp DDI Prediction: A Modeling Network of Rifampicin, Itraconazole, Clarithromycin, Midazolam, Alfentanil, and Digoxin. CPT Pharmacometrics Syst Pharmacol. 2018;7(10):647-659. doi:10.1002/psp4.12343

Published by Lumora Journals · lumora.sa · CC BY 4.0